Rapid Communications

The antiferromagnetic phase of the Floquet-driven Hubbard model

Nicklas Walldorf,[1] Dante M. Kennes,[2] Jens Paaske,[3] and Andrew J. Millis[4,5]

[1]*Center for Nanostructured Graphene (CNG), Department of Physics, Technical University of Denmark, DK-2800 Kongens Lyngby, Denmark*
[2]*Dahlem Center for Complex Quantum Systems and Fachbereich Physik, Freie Universität Berlin, D-14195 Berlin, Germany*
[3]*Center for Quantum Devices, Niels Bohr Institute, University of Copenhagen, DK-2100 Copenhagen, Denmark*
[4]*Department of Physics, Columbia University, 538 West 120th Street, New York, New York 10027, USA*
[5]*Center for Computational Quantum Physics, Flatiron Institute, 162 5th Avenue, New York, New York 10010, USA*

(Received 1 October 2018; revised manuscript received 15 November 2018; published 20 September 2019)

A saddle point plus fluctuation analysis of the periodically driven half-filled two-dimensional Hubbard model is performed. For drive frequencies below the equilibrium gap, we find discontinuous transitions to time-dependent solutions. A highly excited, generically nonthermal distribution of magnons occurs even for drive frequencies far above the gap. Above a critical drive amplitude, the low-energy magnon distribution diverges as the frequency tends to zero and antiferromagnetism is destroyed, revealing the generic importance of collective mode excitations arising from a nonequilibrium drive.

DOI: 10.1103/PhysRevB.100.121110

The rapid development of stable, high-intensity radiation sources has opened up new experimental horizons for the nonequilibrium control of material properties by application of tailored radiation fields [1–3]. An applied radiation field affects a material in two fundamentally different ways: by changing the Hamiltonian, and creating excitations. The former, commonly referred to as "Floquet engineering," offers an exciting route towards engineering new phases of driven matter [4–17]. In some cases (e.g., integrable models with collisionless dynamics) mode excitation can lead to novel dynamical phases [18]. However, in the generic situation, if too many excitations are created, the interesting phases can be destabilized [19–22]. The general consensus in the field has been that if the drive frequency is sufficiently detuned from the electronic transition energies, excitations may be neglected, allowing a focus on Floquet engineering aspects.

In this Rapid Communication we investigate the physics of ac-driven systems with the drive frequency detuned from electronic transitions via a theoretical study of the properties of the Hubbard model. This model is one of the paradigmatic systems of theoretical condensed matter physics, capturing the essential physics of electronic ordering and collective modes. We focus on the effect of the ac drive on the antiferromagnetic phase and the associated collective modes. We find that even in the "detuned case," in which the ac drive does not produce a significant density of quasiparticle excitations, a highly nonequilibrium collective mode distribution is produced, with a remarkable dependence on the drive amplitude suggestive of a dynamical quantum phase transition. Above a critical drive amplitude, the nonequilibrium distribution of collective modes leads to a destruction of long-ranged antiferromagnetic order, possibly even for dimensions higher than two. These findings suggest that collective mode distribution effects may be important more broadly in the physics of Floquet-driven phases.

Model. We consider the situation sketched in Fig. 1: the half-filled two-dimensional square-lattice Hubbard model with nearest-neighbor hopping, repulsive interaction, brought out of equilibrium via an applied electromagnetic field, and tunnel coupled to a metallic reservoir to allow the system to reach a nonequilibrium steady state. The Hamiltonian is

$$\hat{H} = \sum_{\boldsymbol{k}\sigma} \epsilon_{\boldsymbol{k}}(t)\hat{c}^{\dagger}_{\boldsymbol{k}\sigma}\hat{c}_{\boldsymbol{k}\sigma} + U\sum_{i}\hat{n}_{i\uparrow}\hat{n}_{i\downarrow} + \hat{H}_{\rm res}, \qquad (1)$$

where $\epsilon_{\boldsymbol{k}}(t)$ is the electron dispersion and U the on-site repulsion. The operator $\hat{c}^{\dagger}_{i\sigma}$ creates an electron of spin σ at site i of a two-dimensional lattice of unit lattice constant, $c^{\dagger}_{\boldsymbol{k}\sigma}$ is its Fourier transform in the first Brillouin zone, and $\hat{n}_{i\sigma} = \hat{c}^{\dagger}_{i\sigma}\hat{c}_{i\sigma}$. $\hat{H}_{\rm res}$ is a weak tunnel coupling to an infinite-bandwidth reservoir with a flat density of states [23] giving rise to a constant inverse electron lifetime Γ [see Eq. (4) below]. We set the chemical potential corresponding to half filling, set $\hbar = k_B = e = 1$, and include the electric field via the Peierls substitution with a vector potential $A_{x,y}(t) = -E\sin(\Omega t)/\Omega$,

$$\epsilon_{\boldsymbol{k}}(t) = -2\tilde{t}\{\cos[k_x + A_x(t)] + \cos[k_y + A_y(t)]\}. \qquad (2)$$

Henceforth, all energies are given in units of the nearest-neighbor-hopping matrix element $\tilde{t}$.

The equilibrium properties of the model are well understood [24–26]: The ground state is antiferromagnetically (Néel) ordered, has a gap to electronic excitations, and supports gapless spin waves. The thermal population of magnons

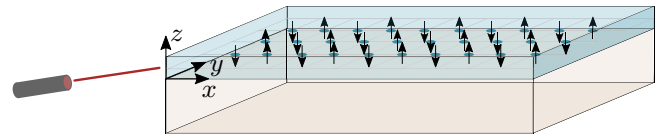

FIG. 1. Sketch of an antiferromagnetically ordered strongly correlated film (top layer, with spins indicated) driven by a radiation field and in contact with a metallic reservoir (bottom layer) kept at thermal equilibrium.

diverges as their energy goes to zero, which in turn leads to the destruction of long-ranged magnetic order at any nonzero temperature in dimension $d \leqslant 2$ [27–29]. These features are revealed by an appropriate interpretation of the results of a conventional mean field plus fluctuation analysis [24,25], which is known to provide a qualitatively correct description of the equilibrium properties of the model.

We study the model for drive frequencies ranging from smaller than the equilibrium gap ("subgap drive regime") to larger than the highest electronic transition visible in linear response ("Magnus drive regime") [5,7,16,30] by solving the nonequilibrium mean-field equations in the presence of a periodic drive and then computing one-loop corrections.

Saddle-point approximation. To generate the mean-field theory we write the model as a Keldysh-contour path integral [31], decouple the interaction via a magnetic-channel Hubbard-Stratonovich field [32] $\boldsymbol{m}$, and consider $\boldsymbol{m}$ to have a mean-field part $m_0 \hat{z} e^{i\boldsymbol{Q}\cdot\boldsymbol{R}_i}$, identified with the Néel order parameter $\boldsymbol{Q} = (\pi, \pi)$, and a fluctuation part $\delta\boldsymbol{m}$, which, when treated to one-loop order, reveals the spin-wave physics.

In a nonequilibrium steady state the mean field is synchronized to the drive [see the inset in Fig. 2(b)] so the mean-field magnetization can be represented as a Fourier series $m_0(t) = \sum_n m_0^{(n)} e^{-in\Omega t}$. The mean-field equation, found as a saddle-point approximation for the classical magnetization field component [33], is then a nonlinear equation for the components $m_0^{(n)}$ of the Floquet-space vector representing $m_0(t)$,

$$m_0^{(n)} = \frac{I}{4\pi N i} {\sum_{\boldsymbol{k}}}' \int_{-\infty}^{\infty} d\omega \, \mathrm{Tr}[\hat{\mathcal{G}}_{\boldsymbol{k},n0}(\omega)(\hat{\tau}_1 \otimes \tau_1 \otimes \sigma_3)], \quad (3)$$

where the primed sum is taken over the magnetic Brillouin zone (BZ), i.e., half of the electronic BZ, $I = U/3$ [32], and $\hat{\mathcal{G}}$, the mean-field Floquet Green's function [34–37], is a matrix in Keldysh ($\hat{\tau}$), momentum-spinor (τ), spin (σ), and Floquet space. The retarded/advanced component of the electron Green's function dressed by the reservoir is given by

$$\mathcal{G}^{R/A\,-1}_{\boldsymbol{k},mn}(\omega) = (\omega + n\Omega \pm i\Gamma)\delta_{mn}\tau_0 \otimes \sigma_0 - h_{\boldsymbol{k},mn}, \quad (4)$$

where $h_{\boldsymbol{k},mn} = \epsilon_{\boldsymbol{k},m-n}\tau_3 \otimes \sigma_0 - m_0^{(m-n)}\tau_1 \otimes \sigma_3$, with $\epsilon_{\boldsymbol{k},m} = \frac{1}{T}\int_{-T/2}^{T/2} dt\, e^{im\Omega t}\epsilon_{\boldsymbol{k}}(t)$, describing electrons driven by the external field and moving in a time-periodic magnetization field. The Keldysh Green's function is given by $\mathcal{G}^K_{\boldsymbol{k},mn}(\omega) = \sum_{m'n'} \mathcal{G}^R_{\boldsymbol{k},mm'}(\omega)\Sigma^K_{\boldsymbol{k},m'n'}(\omega)\mathcal{G}^A_{\boldsymbol{k},n'n}(\omega)$, where $\Sigma^K_{\boldsymbol{k},mn}(\omega) = -2i\Gamma \tanh[(\omega + n\Omega)/2T]\tau_0 \otimes \sigma_0\delta_{mn}$ is the self-energy from coupling to the reservoir. We solve Eqs. (3) and (4) numerically, choosing a Floquet cutoff $|n| \leqslant n_{\max}$, and iterate from an initial guess $m_0^{(n)} = 10^{-2}\theta(n_{\max} - |n|)$. We use the converged solutions as new starting points to explore multistability.

Representative results for the zeroth Floquet component, corresponding to the time-averaged dynamics, are shown in the left-hand panel of Fig. 2. For $I \gg \tilde{t}$ the qualitative physics does not depend on the interaction strength, so we present results only for a single typical case. In the high-frequency ("Magnus") limit $\Omega \gg 2m_0^{(0)}$, theoretical arguments [30] suggest that the system is described by an effective Hamiltonian with the hopping amplitude modified from the equilibrium value. We see that indeed on the mean-field level, the main

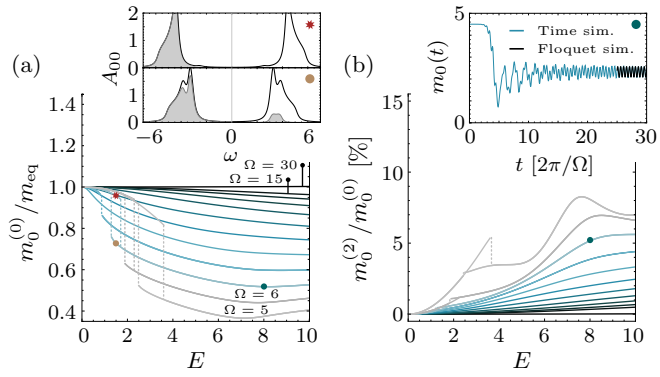

FIG. 2. Mean-field solutions for varying drive frequencies $\Omega =$ 5–15 in steps of 1 as well as $\Omega = 30$. (a) Time-averaged mean field as a function of drive amplitude, and (inset) diagonal component of the time-averaged spectral functions (solid lines) and occupation functions (shaded areas) for the mean-field solutions marked in (a). (b) Second mean-field Floquet component as a function of drive amplitude, and (inset) an explicit time-dependent mean-field solution for $\Omega = 7$ (see Refs. [38,39] for computational details) ramped from the undriven to the driven state synchronized to the time-transformed Floquet mean-field solution. The parameters are $I = 5$, $T = 0.01$, $\Gamma = 0.2$, and $n_{\max} = 10$.

features of the solution remain similar to equilibrium but with parameters renormalized as expected: a magnetic insulating state with the expected [30] small increase in the average staggered magnetization [barely visible in the $\Omega = 30$ trace in Fig. 2(a)] arising from the Magnus-regime renormalization of $\tilde{t}$ by $J_0(E/\Omega)$ [7,16]. However, as the drive frequencies are decreased towards the subgap regime (drive frequency within or below the region of particle-hole continuum excitations) we observe a change to a weak decrease of the order parameter with drive amplitude, and for still lower drive frequency the mean-field equation gives a discontinuous transition (within a regime of bistability) to a state of lower gap amplitude and significant occupation of the upper band [Fig. 2(a) inset]. Within mean-field theory, the state remains magnetically ordered on both sides of the transition; whether a more sophisticated approximation as in Ref. [22] would lead to a Mott or gapless state is an important open question.

Figure 2(b) presents the harmonic content of the order parameter. The spin inversion symmetry of the drive implies that only even harmonics of the drive frequency appear in the order parameter, and we find generically that only the 0 and ± 2 Floquet components have appreciable amplitudes. The resulting 2Ω oscillation in the order parameter implies moderate second harmonic amplitude oscillations in the gap magnitudes [see the inset in Fig. 2(b)]; the resulting nonlinear optical effects will be strongest for incident radiation at frequencies near the gap.

Fluctuations. We now focus on the mean-field solutions at higher drive frequencies, where the density of the electron quasiparticle excitations is negligible. We introduce the fluctuation field as a Keldysh and momentum spinor, $\delta\boldsymbol{m}^{\mu,i}_{\boldsymbol{q}}(t) = [\delta m^{\mu,i}_{\boldsymbol{q}}(t), \delta m^{\mu,i}_{\boldsymbol{q}+\boldsymbol{Q}}(t)]$, with a Keldysh index $i = c, q$ (classical, quantum [31]) and $\mu = \pm$ referring to the directional polar decomposition $x \pm iy$. The fluctuations are

governed by the electron Green's function bubble, which, upon transforming to Floquet space, reads

$$\Pi^{\mu\nu,ij}_{0/Q,\boldsymbol{q},mn}(\omega) = \frac{i}{2N}\sum_{\boldsymbol{k}}{}' \sum_{m'} \int_{-\infty}^{\infty} \frac{d\omega'}{2\pi} \mathrm{Tr}[(\hat{\gamma}_i \otimes \tau_0 \otimes \sigma_\mu) \times \hat{\mathcal{G}}_{\boldsymbol{k},mm'}(\omega')(\hat{\gamma}_j \otimes \tau_{0/1} \otimes \sigma_\nu) \times \hat{\mathcal{G}}_{\boldsymbol{k}+\boldsymbol{q},m'n}(\omega' - \omega - n\Omega)], \quad (5)$$

with Keldysh indices encoded in the matrices $\hat{\gamma}_{c/q} = \hat{\tau}_{0/1}$ [33]. Using the sublattice matrix structure [25]

$$\boldsymbol{\Pi}_{\boldsymbol{q}} = \begin{pmatrix} \Pi_{0,\boldsymbol{q}} & \Pi_{Q,\boldsymbol{q}} \\ \Pi_{Q,\boldsymbol{q}} & \Pi_{0,\boldsymbol{q}+\boldsymbol{Q}} \end{pmatrix}, \quad (6)$$

we define the corresponding transverse fluctuation matrix propagator $\boldsymbol{\chi}^{\perp,ij}_{\boldsymbol{q}}(t,t') = (iN/\pi)\langle \delta m^{+,i}_{\boldsymbol{q}}(t)\delta m^{-,j}_{-\boldsymbol{q}}(t')\rangle$, as

$$\boldsymbol{\chi}^{\perp R/A}_{\boldsymbol{q},mn} = \left[(2I)^{-1} - \boldsymbol{\Pi}^{\perp R/A}_{\boldsymbol{q}}\right]^{-1}_{mn},$$
$$\boldsymbol{\chi}^{\perp K}_{\boldsymbol{q},mn} = \left[(2I)^{-1} - \boldsymbol{\Pi}^{\perp R}_{\boldsymbol{q}}\right]^{-1}_{mm'} \boldsymbol{\Pi}^{\perp K}_{\boldsymbol{q},m'n'} \left[(2I)^{-1} - \boldsymbol{\Pi}^{\perp A}_{\boldsymbol{q}}\right]^{-1}_{n'n}. \quad (7)$$

The time-averaged (00-Floquet) fluctuation spectrum is revealed by $\mathrm{Im}\,\chi^{\perp,R}_{\boldsymbol{0},\boldsymbol{q},00}(\omega)$, shown in the left panel of Fig. 3. We see that the only low-lying excitations are very sharp peaks, corresponding to spin waves, with a small but nonzero broadening from the coupling to the reservoir. The peak energy vanishes and the peak amplitude grows as $\boldsymbol{q} \to \boldsymbol{Q}$. At energies below the charge gap, for positive frequencies $\mathrm{Im}\,\chi^{\perp R}_{\boldsymbol{0},\boldsymbol{q},00}(\omega) \approx Z_q \delta(\omega - \omega_q)$ for not too large Γ. Upon integrating over the peaks in Fig. 3(a), the inverse spectral weight Z_q^{-1} shows a linear $\delta q = |\boldsymbol{q} - \boldsymbol{Q}|$ dependence [Fig. 3(a) inset] which agrees well with the expanded equilibrium result, $Z_q^{-1} \approx \alpha \delta q$, $\alpha = 1/(8\sqrt{2}\pi m_0^2)[2 + t^2/m_0^2 + O(t^4/m_0^4)]$. The ω_q is determined from the peak positions, and gives the dispersions presented in the right panel of Fig. 3. The dispersion exhibits the expected linear momentum dependence at lowest energies, $\omega = v\delta q$. The spin-wave velocity is seen to compare well to the dissipative equilibrium result, $v = (2\sqrt{2}\tilde{t}^2/m_0)(1 - 5\tilde{t}^2/m_0^2 - 3\Gamma/\pi m_0 - \Gamma^2/2m_0^2) + O(\tilde{t}^{2+n}\Gamma^{3-n}/m_0^5)$ for $n = 0, 1, 2, 3$ (consistent with Ref. [26] for $\Gamma = 0$), provided that the hopping amplitude $\tilde{t}$ is replaced by the Magnus-renormalized value $\tilde{t}J_0(E/\Omega)$ [7]. One may view this Bessel-function reduction of the spin-wave velocity as a particularly simple example of Floquet engineering.

The Keldysh component of the transverse propagator contains information about the nonequilibrium distribution of excitations. For low-lying spin waves with $\omega_q \ll \Omega$, this information resides in the zeroth Floquet component, from which we define a time-averaged distribution function F by the ansatz

$$\chi^{\perp K}_{\boldsymbol{0},\boldsymbol{q},00}(\omega) = 2i\,\mathrm{Im}\left[\chi^{\perp R}_{\boldsymbol{0},\boldsymbol{q},00}(\omega)\right] F(\boldsymbol{q},\omega) \approx 2iZ_q\delta(|\omega| - \omega_q)F_q. \quad (8)$$

The spin-wave pole approximation to $\mathrm{Im}\,\chi^R$ allows for a quasiclassical description in terms of an on-shell distribution function $F_q = F(\boldsymbol{q},\omega_q)$ referring only to the mode energy ω_q. In equilibrium, the fluctuation-dissipation theorem (FDT) ensures that $F_q = \coth(\omega_q/2T)$, which tends to unity at $\omega_q \gg T$ and diverges as ω_q^{-1} for $\omega_q \to 0$.

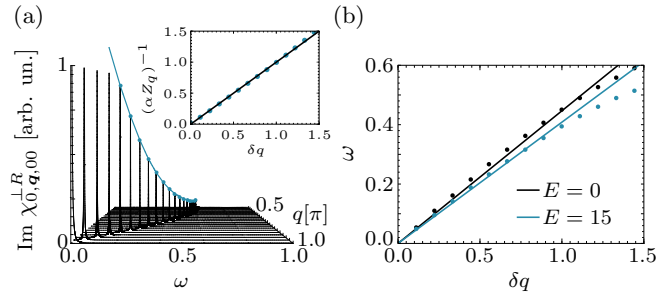

FIG. 3. Transverse spin-wave modes. (a) Imaginary part of the retarded susceptibility as function of frequency and momentum $q_x = q_y = q$ for $E = 15$ showing the spin-wave pole. Inset: Inverse spectral weight of the peaks in (a). (b) Location of the spin-wave pole (points) as a function of frequency and δq together with the equilibrium linear spin-wave dispersion, $\omega = v\delta q$, (solid lines) with $\tilde{t} \to \tilde{t}J_0(E/\Omega)$. The parameters are $I = 5$, $\Omega = 30$, $T = 0.01$, $\Gamma = 0.2$, and $n_{\max} = 3$.

Figure 4(a) shows the inverse distribution function F_q^{-1} as a function of the mode energy ω_q at different drive amplitudes for a low reservoir temperature $T = 0.01$. We plot the reciprocal to fit all data on the same panel. Because the reservoir temperature is substantially lower than the lowest ω_q included in our numerics, the equilibrium F_q [Fig. 4(b)] is indistinguishable from unity. We see that increasing the drive amplitude increases F_q (decreases F_q^{-1}) at all ω_q, with a larger increase for lower ω_q. Increasing either the drive frequency Ω or the reservoir coupling Γ for fixed drive amplitude reduces F_q (open symbols, left panel of Fig. 4). For higher ω_q, F_q initially increases rapidly as the drive amplitude increases, but then saturates as the amplitude becomes large. For small ω_q, the situation is different. For the two weakest drive amplitudes, F_q appears to approach a finite, nonzero value as ω_q approaches zero; for the intermediate drive amplitude, F_q^{-1} vanishes linearly as $\omega_q \to 0$, while for the two highest drive amplitudes, F_q^{-1} vanishes faster than linearly as $\omega_q \to 0$.

Apart from the intermediate drive amplitude ($E = 3$), these distribution functions depart markedly from the equilibrium distribution dictated by the FDT. To illustrate this more clearly, Fig. 4(c) shows the effective temperature T_{eff} as defined by $F_q = \coth[\omega_q/2T_{\mathrm{eff}}(q)]$. We see that the results fall into two groups. For the two smallest drive amplitudes, T_{eff} is larger at high ω_q (a very substantial excitation of high q spin waves above the equilibrium value), but decreases to a value consistent with the reservoir temperature as $\omega_q \to 0$. For the intermediate drive amplitude, $T_{\mathrm{eff}} \approx 0.66$ is essentially momentum-independent (i.e. F_q fits well to the equilibrium form) and much larger than the reservoir temperatures. For the two larger drive amplitudes, T_{eff} increases rapidly for small ω_q, indicating a superthermal occupancy of the low-lying spin-wave modes, in other words, F_q diverging faster than $1/\omega_q$.

The site- and period-averaged mean-squared fluctuations of the classical component of the order parameter are given by

$$\langle |\delta m^{+,c}|^2 \rangle = \frac{1}{N}\sum_{\boldsymbol{q}} \int \frac{d\omega}{4\pi i} \chi^{\perp K}_{0,\boldsymbol{q},00}(\omega) \sim \int \frac{d^2q}{(2\pi)^2} Z_q F_q. \quad (9)$$

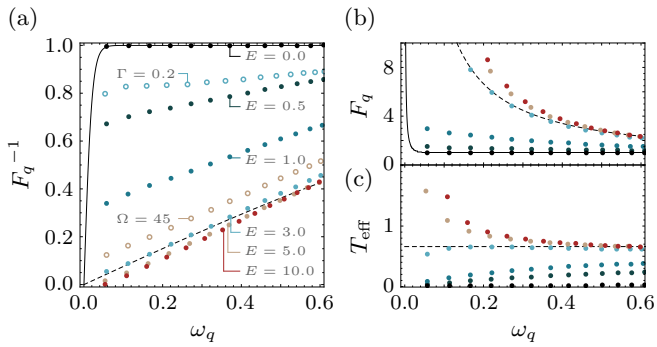

FIG. 4. (a) F_q^{-1} and (b) F_q as functions of ω_q for increasing drive amplitude with $\Gamma = 0.02$ and $\Omega = 30$ together with the equilibrium curves for $T = 0.01$ (solid) and $T = 0.66$ (dashed). In (a) is also shown the result for $\Omega = 45$, $E = 5.0$, $\Gamma = 0.02$ and $\Gamma = 0.2$, $E = 3.0$, $\Omega = 30$. (c) $T_{\rm eff}$ corresponding to the curves in (b) together with the equilibrium $T = 0.66$ line (dashed). The parameters are $I = 5$, $T = 0.01$, and $n_{\rm max} = 3$.

In thermal equilibrium at any nonzero temperature, both F_q and Z_q diverge as $1/\delta q$, and $\langle|\delta m^{+,c}|^2\rangle$ therefore diverges logarithmically with system size in two dimensions. This is the expression in the one-loop calculation of the well-known result [27,28] that thermal fluctuations destabilize long-ranged magnetic order in continuous-symmetry systems of dimension $d \leqslant 2$. Our results indicate that the generalization to systems out of equilibrium is richer than expected from previous work. Unlike the dc current-driven ferromagnetic case [20,21], a weak nonequilibrium drive would not destabilize the ordered state for $d = 2$, but larger drives lead to a superthermal occupancy that can destabilize the order even in $d > 2$.

Conclusions. We have used a mean field plus fluctuation analysis of the antiferromagnetic two-dimensional Hubbard model driven by an oscillating electric field to examine the accepted theoretical intuition, which suggests that if an ac drive is detuned from direct electronic transition energies, its main effect is to renormalize Hamiltonian parameters. Our solution of the full nonequilibrium problem shows rich additional physics: (i) In the subgap drive regime, the drive is found to induce a substantial time-dependent component of the order parameter with first-order-like transitions and coexistence regimes involving several locally stable (at least at the mean-field level) phases, and (ii) in all cases, including the "Magnus" regime of very-high-frequency drive where the basic electronic state evolves smoothly with the drive amplitude and no electronic quasiparticle excitations are created, we find a highly nonthermal distribution of magnons. Whereas the main focus in this Rapid Communication is on the latter, an analysis of fluctuation effects on the bistability observed in the subgap drive regime is an interesting open question.

The interaction-mediated transfer of energy to the spin fluctuations may be thought of as a spin-charge coupling (albeit a weaker kind than considered, e.g., in Ref. [40]). The dependence of the magnon distribution on the drive frequency and coupling to the reservoir indicates that the pathway to spin-wave excitation involves reservoir states. The kinetics of this process, and the generalization to more realistic models of solids, are an important subject for future research. The distribution of fluctuations depends in a remarkable way on the drive amplitude. For small and moderate drive amplitudes, there is substantial excitation of higher-energy modes, but as the momentum tends to the ordering wave vector, the distribution tends towards the equilibrium one. However, at larger drive amplitudes, the distribution diverges faster than ω_q^{-1} as momentum tends towards the ordering wave vector, which would indicate destabilization of order even in three dimensions. This apparent dynamical phase transition as a function of drive amplitude requires further study.

More generally, our findings show that the low-lying collective degrees of freedom are generically excited by the drive, and have a large, typically nonthermal, and drive amplitude-dependent occupancy that can lead to remarkable effects on physical properties. This finding calls into question the Floquet engineering paradigm in which applied radiation changes the Hamiltonian without changing the distribution function.

Acknowledgments. The Center for Nanostructured Graphene (Project DNRF103) and the Center for Quantum Devices are sponsored by the Danish National Research Foundation. A.J.M. and D.M.K. were supported by the US Department of Energy, Office of Basic Energy Sciences, Division of Materials Sciences and Engineering Grant No. DE SC0018218. D.M.K. additionally acknowledges support by the Deutsche Forschungsgemeinschaft through the Emmy Noether program (KA 3360/2-1). N.W. thanks Antti-Pekka Jauho for useful discussions.

[1] R. Mankowsky, M. Först, and A. Cavalleri, Non-equilibrium control of complex solids by nonlinear phononics, Rep. Prog. Phys. **79**, 064503 (2016).

[2] D. N. Basov, R. D. Averitt, and D. Hsieh, Towards properties on demand in quantum materials, Nat. Mater. **16**, 1077 (2017).

[3] Y. Tokura, M. Kawasaki, and N. Nagaosa, Emergent functions of quantum materials, Nat. Phys. **13**, 1056 (2017).

[4] M. S. Rudner, N. H. Lindner, E. Berg, and M. Levin, Anomalous Edge States and the Bulk-Edge Correspondence for Periodically Driven Two-Dimensional Systems, Phys. Rev. X **3**, 031005 (2013).

[5] M. Bukov, L. D'Alessio, and A. Polkovnikov, Universal high-frequency behavior of periodically driven systems: From dynamical stabilization to Floquet engineering, Adv. Phys. **64**, 139 (2015).

[6] R. Singla, G. Cotugno, S. Kaiser, M. Först, M. Mitrano, H. Y. Liu, A. Cartella, C. Manzoni, H. Okamoto, T. Hasegawa, S. R. Clark, D. Jaksch, and A. Cavalleri, THz-Frequency Modulation of the Hubbard U in an Organic Mott Insulator, Phys. Rev. Lett. **115**, 187401 (2015).

[7] J. H. Mentink, K. Balzer, and M. Eckstein, Ultrafast and reversible control of the exchange interaction in Mott insulators, Nat. Commun. **6**, 6708 (2015).

[8] M. Claassen, C. Jia, B. Moritz, and T. P. Devereaux, All-optical materials design of chiral edge modes in transition-metal dichalcogenides, Nat. Commun. **7**, 13074 (2016).

[9] M. Knap, M. Babadi, G. Refael, I. Martin, and E. Demler, Dynamical Cooper pairing in nonequilibrium electron-phonon systems, Phys. Rev. B **94**, 214504 (2016).

[10] D. A. Abanin, W. De Roeck, W. W. Ho, and F. Huveneers, Effective Hamiltonians, prethermalization, and slow energy absorption in periodically driven many-body systems, Phys. Rev. B **95**, 014112 (2017).

[11] D. M. Kennes, E. Y. Wilner, D. R. Reichman, and A. J. Millis, Transient superconductivity from electronic squeezing of optically pumped phonons, Nat. Phys. **13**, 479 (2017).

[12] M. A. Sentef, Light-enhanced electron-phonon coupling from nonlinear electron-phonon coupling, Phys. Rev. B **95**, 205111 (2017).

[13] Y. Murakami, N. Tsuji, M. Eckstein, and P. Werner, Nonequilibrium steady states and transient dynamics of conventional superconductors under phonon driving, Phys. Rev. B **96**, 045125 (2017).

[14] J. R. Coulthard, S. R. Clark, S. Al-Assam, A. Cavalleri, and D. Jaksch, Enhancement of superexchange pairing in the periodically driven Hubbard model, Phys. Rev. B **96**, 085104 (2017).

[15] S. Kitamura, T. Oka, and H. Aoki, Probing and controlling spin chirality in Mott insulators by circularly polarized laser, Phys. Rev. B **96**, 014406 (2017).

[16] D. M. Kennes, A. de la Torre, A. Ron, D. Hsieh, and A. J. Millis, Floquet Engineering in Quantum Chains, Phys. Rev. Lett. **120**, 127601 (2018).

[17] N. Tancogne-Dejean, M. A. Sentef, and A. Rubio, Ultrafast Modification of Hubbard U in a Strongly Correlated Material: *Ab Initio* High-Harmonic Generation in NiO, Phys. Rev. Lett. **121**, 097402 (2018).

[18] H. P. Ojeda Collado, J. Lorenzana, G. Usaj, and C. A. Balseiro, Population inversion and dynamical phase transitions in a driven superconductor, Phys. Rev. B **98**, 214519 (2018).

[19] F. Peronaci, M. Schiro, and O. Parcollet, Resonant Thermalization of Periodically Driven Strongly Correlated Electrons, Phys. Rev. Lett. **120**, 197601 (2018).

[20] A. Mitra, S. Takei, Y. B. Kim, and A. J. Millis, Nonequilibrium Quantum Criticality in Open Electronic Systems, Phys. Rev. Lett. **97**, 236808 (2006).

[21] A. Mitra and A. J. Millis, Current-driven quantum criticality in itinerant electron ferromagnets, Phys. Rev. B **77**, 220404(R) (2008).

[22] J. Jose Mendoza-Arenas, F. Javier Gomez-Ruiz, M. Eckstein, D. Jaksch, and S. R. Clark, Ultra-fast control of magnetic relaxation in a periodically driven Hubbard model, Ann. Phys. **529**, 1700024 (2017).

[23] For details on the coupling to an infinite-bandwidth flat-band reservoir and how it leads to broadening, see, e.g., Ref. [41].

[24] J. R. Schrieffer, X.-G. Wen, and S.-C. Zhang, Spin-Bag Mechanism of High-Temperature Superconductivity, Phys. Rev. Lett. **60**, 944 (1988).

[25] J. R. Schrieffer, X. G. Wen, and S. C. Zhang, Dynamic spin fluctuations and the bag mechanism of high-T_c superconductivity, Phys. Rev. B **39**, 11663 (1989).

[26] A. Singh, Spin-wave spectral properties of the Mott-Hubbard antiferromagnet: The intermediate-coupling regime, Phys. Rev. B **48**, 6668 (1993).

[27] P. C. Hohenberg, Existence of long-range order in one and two dimensions, Phys. Rev. **158**, 383 (1967).

[28] N. D. Mermin and H. Wagner, Absence of Ferromagnetism or Antiferromagnetism in One- or Two-Dimensional Isotropic Heisenberg Models, Phys. Rev. Lett. **17**, 1133 (1966).

[29] A. Auerbach, *Interacting Electrons and Quantum Magnetism* (Springer, Berlin, 1998).

[30] W. Magnus, On the exponential solution of differential equations for a linear operator, Commun. Pure Appl. Math. **7**, 649 (1954).

[31] A. Kamenev, *Field Theory of Non-Equilibrium Systems* (Cambridge University Press, Cambridge, UK, 2011).

[32] P. Coleman, *Introduction to Many-Body Physics* (Cambridge University Press, Cambridge, UK, 2015).

[33] A. Kamenev and A. Levchenko, Keldysh technique and nonlinear sigma-model: Basic principles and applications, Adv. Phys. **58**, 197 (2009).

[34] T. Kitagawa, T. Oka, A. Brataas, L. Fu, and E. Demler, Transport properties of nonequilibrium systems under the application of light: Photoinduced quantum Hall insulators without Landau levels, Phys. Rev. B **84**, 235108 (2011).

[35] H. Aoki, N. Tsuji, M. Eckstein, M. Kollar, T. Oka, and P. Werner, Nonequilibrium dynamical mean-field theory and its applications, Rev. Mod. Phys. **86**, 779 (2014).

[36] A. K. Eissing, V. Meden, and D. M. Kennes, Renormalization in Periodically Driven Quantum Dots, Phys. Rev. Lett. **116**, 026801 (2016).

[37] D. M. Kennes, Transport through periodically driven correlated quantum wires, arXiv:1801.02866.

[38] D. M. Kennes, S. G. Jakobs, C. Karrasch, and V. Meden, Renormalization group approach to time-dependent transport through correlated quantum dots, Phys. Rev. B **85**, 085113 (2012).

[39] D. M. Kennes and V. Meden, Quench dynamics of correlated quantum dots, Phys. Rev. B **85**, 245101 (2012).

[40] F. Dolcini, Signature of interaction in dc transport of ac-gated quantum spin Hall edge states, Phys. Rev. B **85**, 033306 (2012).

[41] S. Takei, Dissipation and decoherence in open nonequilibrium electronic systems, Ph.D. thesis, University of Toronto, 2008.